

Bispectrum Unbiasing for Dilation-Invariant Multi-reference Alignment

Liping Yin^{*}, Anna Little[†], and Matthew Hirn[‡]

CMSE Department and Mathematics Department, Michigan State University^{*‡}

Department of Mathematics and the Utah Center For Data Science, University of Utah[†]

Email: ^{*}yinlipi1@msu.edu, [†]little@math.utah.edu, [‡]mhirn@msu.edu

Abstract—Motivated by modern data applications such as cryo-electron microscopy, the goal of classic multi-reference alignment (MRA) is to recover an unknown signal $f : \mathbb{R} \rightarrow \mathbb{R}$ from many observations that have been randomly translated and corrupted by additive noise. We consider a generalization of classic MRA where signals are also corrupted by a random scale change, i.e. dilation. We propose a novel data-driven unbiasing procedure which can recover an unbiased estimator of the bispectrum of the unknown signal, given knowledge of the dilation distribution. Lastly, we invert the recovered bispectrum to achieve full signal recovery, and validate our methodology on a set of synthetic signals.

I. INTRODUCTION TO MRA

In classic multi-reference alignment (MRA), one seeks to recover an unknown signal $f : \mathbb{R} \rightarrow \mathbb{R}$ from many observations that have been randomly translated and corrupted by additive noise. The MRA problem is a simplified version of problems in cryo-electron microscopy (cryo-EM), and is similar to problems in other fields such as structural biology [16], [36], [37], [41], [42], [45], image registration [8], [19], and image processing [48]. A formal description of the assumptions is given in Model 1.

Model 1 (Classic MRA). Suppose we have M independent observations of a real-valued function $f \in L^2(\mathbb{R})$ defined by

$$y_j(x) = f(x - t_j) + \varepsilon_j(x), \quad 1 \leq j \leq M,$$

where

- (i) $\text{supp}(y_j) \subset [-\frac{1}{2}, \frac{1}{2}]$ for $1 \leq j \leq M$.
- (ii) $\{t_j\}_{j=1}^M$ are independent samples of a random variable $t \in \mathbb{R}$.
- (iii) $\{\varepsilon_j(x)\}_{j=1}^M$ are independent white noise processes on $[-\frac{1}{2}, \frac{1}{2}]$ with variance σ^2 .

Methods for solving Model 1 can be grouped into two categories. The first approach is synchronization methods [2], [3], [4], [5], [7], [12], [13], [39], [44], [47], which try to recover each translation factor $\{t_j\}_{j=1}^M$, align the signals using the recovered translation factor,

and average the aligned signals to get a smoother estimate for the ground truth signal. However, synchronization methods can be problematic when the signal-to-noise ratio (SNR) is small. Although synchronization is tenable at small noise levels, at high noise levels, the peaks are not recognizable and synchronization fails. The second approach involves estimating the signal directly, without estimation of the translation factors, using ideas such as the method of moments [21], [26], [43]. The method of invariants [2], [6], [14], [24], [23] is an important subclass of such methods in which one first estimates translation invariant features of the hidden signal (for example its power spectrum and bispectrum), and then an inversion algorithm is applied to recover the hidden signal from the estimated features. Expectation maximization (EM) algorithms [1], [15] have also shown success for signal recovery, although potential disadvantages include high computation time and convergence to local minima.

Although analysis of Model 1 has led to important insights [38], it is a highly simplified model which does not include important sources of physical variation in many modern applications. For example, in three dimensional applications such as cryo-EM, molecules are randomly rotated and one only has access to 2D projections of the molecule. In addition, objects may undergo changes in size/scale, as well as non-static regions where macromolecular structures “flop” around [30], [17], [29], [18]. One can think of these deformations as a diffeomorphism acting on the molecule before retrieving the observations. In other words, if g is a function extracting the observations and x is a molecule, we retrieve $g(\xi(x))$, where $\xi \in C^2(\mathbb{R}^n)$ has a bijective, continuous hessian. However solving Model 1 in the presence of random diffeomorphisms is highly challenging, and generally must involve either assuming that the diffeomorphism is “small”, or that it has an underlying structure which can be leveraged. In this article, we pursue the latter approach, and specifically focus on the case where the diffeomorphism is a linear function, i.e. the hidden signal is also randomly dilated. As further motivation, we note the analysis of dilations is important in imaging [10],

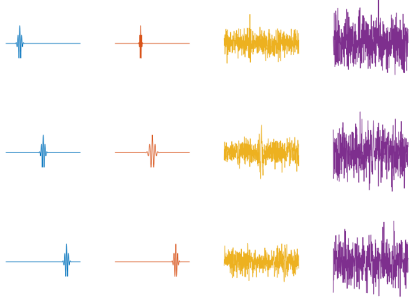


Fig. 1: **Left Column:** three ground truth signals that have been translated without any additive noise. **Middle Left Column:** Dilating each of the signals. **Middle Right Column:** Adding Gaussian noise with $\sigma^2 = 0.5$ to each of the signals. **Right Column:** Adding Gaussian noise with $\sigma^2 = 2$ to each of the signals. Source: [24].

[9], [46], [25], [32], [40] and audio [34], [35], [33], [34], [35], [33] applications. Incorporating dilations into Model 1 leads to the formulation of Model 2 below; see Figure 1 for an illustration.

Model 2. Suppose we have M independent observations of a real-valued function $f \in L^2(\mathbb{R})$ defined by

$$\begin{aligned} y_j(x) &:= f((1 - \tau_j)^{-1}(x - t_j)) + \varepsilon_j(x) \\ &:= f_j(x) + \varepsilon_j(x), \quad 1 \leq j \leq M. \end{aligned}$$

Furthermore, assume that

- (i) $\text{supp}(y_j) \subset [-\frac{1}{2}, \frac{1}{2}]$ for $1 \leq j \leq M$.
- (ii) $\{t_j\}_{j=1}^M$ are independent samples of a random variable $t \in \mathbb{R}$.
- (iii) $\{\tau_j\}_{j=1}^M$ are independent samples of a uniformly distributed random variable $\tau \in \mathbb{R}$ satisfying $\mathbb{E}[\tau] = 0$ and $\text{Var}(\tau) = \eta^2 \leq \frac{1}{12}$.
- (iv) $\{\varepsilon_j(x)\}_{j=1}^M$ are independent white noise processes on $[-\frac{1}{2}, \frac{1}{2}]$ with variance σ^2 .

Although Model 2 corresponds to the simplest possible class of diffeomorphisms other than translations (i.e. linear functions), solving Model 2 is significantly more difficult than solving Model 1, as even small dilations can create large perturbations in the frequency domain, especially for high frequency signals [31]. Our solution to this problem will be a method of invariants which utilizes translation invariant Fourier features such as the power spectrum and bispectrum. However, since the Fourier Transform modulus is unstable to small dilations, we must unbiased the Fourier invariants to remove the impact of dilations before inversion.

Model 2 was also considered in [23], [24]. However both papers only propose estimators for the *power spectrum* of the hidden signal and thus do not fully solve Model 2. [23] use wavelet-based invariants and

a differential unbiasing procedure, but the method fails to produce a fully unbiased estimator of the power spectrum. [24] develop a novel unbiasing technique which can be applied to the noisy power spectra to obtain a fully unbiased power spectrum estimator. In this article we develop a similar unbiasing procedure that yields an unbiased estimator of the *bispectrum* of the hidden signal. Since the bispectrum is invertible under fairly general conditions, we thus provide the first method capable of achieving full signal recovery for Model 2.

For convenience we also define the following noiseless model, Model 3, given by:

Model 3. Suppose we have M independent observations of a function real-valued $f \in L^2(\mathbb{R})$ defined by

$$f_j(x) = f((1 - \tau_j)^{-1}(x - t_j)), \quad 1 \leq j \leq M$$

Furthermore, assume that

- (i) $\text{supp}(f_j) \subset [-\frac{1}{2}, \frac{1}{2}]$ for $1 \leq j \leq M$.
- (ii) $\{t_j\}_{j=1}^M$ are independent samples of a random variable $t \in \mathbb{R}$.
- (iii) $\{\tau_j\}_{j=1}^M$ are independent samples of a uniformly distributed random variable $\tau \in \mathbb{R}$ with $\mathbb{E}[\tau] = 0$ and $\text{Var}(\tau) = \eta^2 \leq \frac{1}{12}$.

We note that solving Model 3 is in fact trivial, since in the absence of additive noise one can first estimate $\|f\|_2$ and then recover f (up to translation) by an appropriate dilation of any observation. However to solve Model 2, it is convenient to first solve Model 3 via Fourier invariants and then generalize the approach to the noisy setting.

The remainder of the article is organized as follows. Section II establishes necessary notation and definitions. Section III gives bispectrum recovery results for Model 3. Section IV gives bispectrum recovery results for Model 2. Section V discusses how the proposed method can be implemented by solving a convex optimization problem. Section VI reports numerical experiments investigating the accuracy of bispectrum recovery, and Section VII reports numerical experiments investigating the accuracy of full hidden signal recovery. Section VIII concludes the article.

II. NOTATION AND PRELIMINARIES

We let $L^q(\mathbb{R})$ represent the set of functions f such that $\|f\|_q^q = \int_{\mathbb{R}} |f|^q dx < \infty$. The Fourier Transform of $f \in L^1(\mathbb{R})$ is

$$\hat{f}(\omega) = \int_{\mathbb{R}} f(t)e^{-i\omega t} dt, \quad (1)$$

the power spectrum is

$$(Pf)(\omega) = |\hat{f}(\omega)|^2, \quad (2)$$

and the bispectrum is

$$Bf(\omega_1, \omega_2) = \hat{f}(\omega_1)\hat{f}^*(\omega_2)\hat{f}(\omega_2 - \omega_1), \quad (3)$$

where h^* denotes the complex conjugate of h . Let $g := Bf$ where f is the hidden signal. For the second and third models, let

$$g_\eta(\omega_1, \omega_2) := \mathbb{E}_\tau[(Bf_j)(\omega_1, \omega_2)].$$

We will also define the following constants and operations used in the rest of the paper:

$$C_0 := \frac{(1 - \sqrt{3}\eta)}{(1 + \sqrt{3}\eta)}, \quad C_1 := 2\sqrt{3}\eta, \quad C_2 := \frac{1}{1 + \sqrt{3}\eta}. \quad (4)$$

Additionally, define the dilation operator

$$L_C g(\omega_1, \omega_2) := C^4 g(C\omega_1, C\omega_2).$$

Note that in polar coordinates (r, θ) , we have $L_C g(r, \theta) = C^4 g(Cr, \theta)$. To precisely quantify higher order error terms, we define the following functions:

$$(\overline{Bf})^k(r, \theta) := r^k \max_{\alpha \in [r/2, 2r]} |\partial_\alpha^k (Bf)(\alpha, \theta)|$$

for integer k . Throughout the paper we write $f \lesssim g$ when $f \leq Cg$ for an absolute constant C . We write $f \lesssim_\alpha g$ or $f = O_\alpha(g)$ when $f \leq C_\alpha g$ for a constant C depending on α .

III. BISPECTRUM RECOVERY FOR MODEL 3

We first illustrate how to define an unbiased estimator for the bispectrum under Model 3, i.e. in the absence of additive noise. As in [24], it is insightful to first consider the case where we have an infinite number of samples and thus perfect access to g_η . In this case the bispectrum of the hidden signal can be perfectly recovered, assuming η is known, as described in the following theorem.

Theorem 1. *Assume that $Bf \in C^1(\mathbb{R}^2)$. Then Bf can be recovered from g_η , namely:*

$$Bf(r, \theta) = (I - L_{C_0})^{-1} C_1 L_{C_2} \left(4g_\eta(r, \theta) + r \frac{\partial g_\eta}{\partial r}(r, \theta) \right).$$

Proof. Recall that the Bispectrum is given by

$$Bf(\omega_1, \omega_2) = \hat{f}(\omega_1) \hat{f}^*(\omega_2) \hat{f}(\omega_2 - \omega_1).$$

The Fourier Transform of each f_j is $e^{-i\omega t_j} (1 - \tau_j) \hat{f}((1 - \tau_j)\omega)$, so

$$(Bf_j)(\omega_1, \omega_2) = (1 - \tau_j)^3 (Bf)((1 - \tau_j)\omega_1, (1 - \tau_j)\omega_2).$$

Since τ has uniform distribution with variance η^2 , the pdf of τ has form $p_\tau = \frac{1}{2\sqrt{3}\eta} \chi_{[-\sqrt{3}\eta, \sqrt{3}\eta]}$. Thus:

$$\begin{aligned} g_\eta(\omega_1, \omega_2) &= \mathbb{E}_\tau [Bf_j(\omega_1, \omega_2)] \\ &= \mathbb{E}_\tau [(1 - \tau)^3 g((1 - \tau)\omega_1, (1 - \tau)\omega_2)] \\ &= \int (1 - \tau)^3 g((1 - \tau)\omega_1, (1 - \tau)\omega_2) p_\tau(\tau) d\tau. \end{aligned}$$

Now we convert to polar coordinates (r, θ) and let $\tilde{\tau} = (1 - \tau)r$:

$$\begin{aligned} g_\eta(r, \theta) &= \frac{1}{2\sqrt{3}\eta} \int_{-\sqrt{3}\eta}^{\sqrt{3}\eta} (1 - \tau)^3 g((1 - \tau)r, \theta) d\tau \\ &= \frac{1}{2\sqrt{3}\eta r^4} \int_{(1 - \sqrt{3}\eta)r}^{(1 + \sqrt{3}\eta)r} \tilde{\tau}^3 g(\tilde{\tau}, \theta) d\tilde{\tau}. \end{aligned}$$

Let H be the antiderivative in the variable w for the function $h(w, \theta) = w^3 g(w, \theta)$. In other words,

$$\frac{\partial H}{\partial w}(w, \theta) = h(w, \theta) = w^3 g(w, \theta).$$

By Fundamental Theorem of Calculus,

$$2\sqrt{3}\eta r^4 g_\eta(r, \theta) = H((1 + 3\sqrt{\eta})r, \theta) - H((1 - 3\sqrt{\eta})r, \theta).$$

Now take derivative with respect to r and divide both sides by r^3 to get

$$\begin{aligned} &2\sqrt{3}\eta \left(4g_\eta(r, \theta) + r \frac{\partial g_\eta}{\partial r}(r, \theta) \right) \\ &= (1 + 3\sqrt{\eta})^4 g((1 + 3\sqrt{\eta})r, \theta) \\ &\quad - (1 - 3\sqrt{\eta})^4 g((1 - 3\sqrt{\eta})r, \theta). \end{aligned}$$

We now apply the dilation operation L_{C_2} to both sides and rewrite the right side in terms of I and L_{C_0} to get

$$C_1 L_{C_2} \left(4g_\eta(r, \theta) + r \frac{\partial g_\eta}{\partial r}(r, \theta) \right) = (I - L_{C_0})g(r, \theta).$$

Thus:

$$g(r, \theta) = (I - L_{C_0})^{-1} C_1 L_{C_2} \left(4g_\eta(r, \theta) + r \frac{\partial g_\eta}{\partial r}(r, \theta) \right). \quad \square$$

In the finite sample case, g_η is not known, but under Model 3 it can be well approximated by:

$$\tilde{g}_\eta(\omega_1, \omega_2) := \frac{1}{M} \sum_{j=1}^M (Bf_j)(\omega_1, \omega_2).$$

Motivated by Theorem 1, we thus define the following estimator:

$$\begin{aligned} &(\widetilde{Bf})(r, \theta) \\ &:= (I - L_{C_0})^{-1} C_1 L_{C_2} \left(4\tilde{g}_\eta(r, \theta) + r \frac{\partial \tilde{g}_\eta}{\partial r}(r, \theta) \right). \end{aligned} \quad (5)$$

To show the estimator \widetilde{Bf} has a small error, we will need the following lemma, which is a straight-forward generalization of Lemma 1 in [24].

Lemma 1. *Assume $Bf \in C^1(\mathbb{R})$ and \widetilde{Bf} is as defined in (5). Then*

$$\begin{aligned} \|Bf(r, \theta) - \widetilde{Bf}(r, \theta)\|_2^2 &\lesssim \|g_\eta(r, \theta) - \tilde{g}_\eta(r, \theta)\|_2^2 \\ &\quad + \|r \partial_r g_\eta(r, \theta) - r \partial_r \tilde{g}_\eta(r, \theta)\|_2^2. \end{aligned}$$

This lemma implies that bounding the mean squared error (MSE) of \widetilde{Bf} reduces to bounding the MSE of \widetilde{g}_η and $r\partial_r\widetilde{g}_\eta$; since these estimators are unbiased and based off of M samples, standard arguments show the MSE converges to 0 at rate $O_f(\frac{\eta^2}{M})$ as described in the next theorem.

Theorem 2. *Let \widetilde{Bf} be as in (5) and assume that $Bf \in C^3(\mathbb{R}^2)$ and $(\overline{Bf})^k \in L^2(\mathbb{R}^2)$ for $k = 2, 3$. Then:*

$$\begin{aligned} & \mathbb{E} \left[\|Bf - \widetilde{Bf}\|_2^2 \right] \\ & \lesssim \frac{\eta^2}{M} \|(Bf)(r, \theta)\|_2^2 + \frac{\eta^2}{M} \|r\partial_r(Bf)(r, \theta)\|_2^2 \\ & + \frac{\eta^2}{M} \|r^2\partial_{rr}(Bf)(r, \theta)\|_2^2 + O_f \left(\frac{\eta^4}{M} \right). \end{aligned}$$

Proof. See Appendix A. \square

We remark that when the dilations are large and/or the hidden signal is high frequency, the empirical average \widetilde{g}_η is an extremely distorted approximation of Bf , but the unbiasing procedure defined in (5) produces a very accurate estimator \widetilde{Bf} ; see Figure 4.

IV. BISPECTRUM RECOVERY FOR MODEL 2

Having successfully recovered the bispectrum under Model 3, we now extend the approach to the noisy setting, i.e. Model 2. The additive noise creates additional difficulties. First, if we compute the MSE on \mathbb{R}^2 as is done in Theorem 2, it will diverge. Second, we no longer have access to \widetilde{g}_η , but only to

$$\frac{1}{M} \sum_{j=1}^M By_j.$$

Finally, the empirical average of the bispectra is no longer smooth due to the additive noise, and thus cannot be differentiated as done in (5).

To deal with the first challenge, we compute the MSE on a finite domain Ω . To deal with the second challenge, we first perform a σ -based centering to unbias the bispectra for the additive noise. More specifically, we define

$$\begin{aligned} R_\sigma(\omega_1, \omega_2) := & \tilde{\mu}(\omega_1)h(\omega_1) + \tilde{\mu}^*(\omega_2)h(\omega_2) \\ & + \tilde{\mu}(\omega_2 - \omega_1)h(\omega_2 - \omega_1), \end{aligned} \quad (6)$$

where $h(\omega) = 2\sigma^2 \frac{\sin(\frac{1}{2}\omega)}{\omega}$ for $\omega \neq 0$, $h(0) = \sigma^2$, and $\tilde{\mu}(\omega) = \frac{1}{M} \sum_{j=1}^M \hat{y}_j(\omega)$ approximates $\mu(\omega) = \mathbb{E}_\tau[\hat{f}_j(\omega)]$. We establish this is the correct additive noise unbiasing term in the next lemma.

Lemma 2. *Assume Model 2 and R_σ as in (6). Then:*

$$\mathbb{E}_{\tau, \epsilon}[By_j - R_\sigma] = \mathbb{E}_\tau[Bf_j] = g_\eta.$$

Proof. Since ε_j is a white noise process on $[-1/2, 1/2]$ with variance σ^2 , we can write $\hat{\varepsilon}_j(\omega) = \int_{-1/2}^{1/2} e^{-i\omega x} dB_x$ as an integral with respect to a Brownian motion, and it is clear that terms involving an odd power of $\hat{\varepsilon}_j$ are mean zero. Thus for fixed τ_j :

$$\begin{aligned} & \mathbb{E}_\varepsilon[By_j(\omega_1, \omega_2)] \\ & = Bf_j(\omega_1, \omega_2) + \mathbb{E}_\varepsilon[\hat{f}_j(\omega_1)\hat{\varepsilon}_j^*(\omega_2)\hat{\varepsilon}_j(\omega_2 - \omega_1) \\ & + \hat{f}_j^*(\omega_2)\hat{\varepsilon}_j(\omega_1)\hat{\varepsilon}_j(\omega_2 - \omega_1) + \hat{\varepsilon}_j(\omega_1)\hat{\varepsilon}_j^*(\omega_2)\hat{f}_j(\omega_2 - \omega_1)] \\ & = Bf_j(\omega_1, \omega_2) + \hat{f}_j(\omega_1)h(\omega_1) \\ & + \hat{f}_j^*(\omega_2)h(\omega_2) + \hat{f}_j(\omega_2 - \omega_1)h(\omega_2 - \omega_1) \end{aligned}$$

since $\mathbb{E}_\varepsilon[\hat{\varepsilon}(\omega_1)\hat{\varepsilon}^*(\omega_2)] = h(\omega_2 - \omega_1)$ (see Theorem 4.5 of [27]). Taking expectation over τ now gives:

$$\begin{aligned} \mathbb{E}_{\tau, \epsilon}[By_j] & = g_\eta + \mu(\omega_1)h(\omega_1) + \mu^*(\omega_2)h(\omega_2) \\ & + \mu(\omega_2 - \omega_1)h(\omega_2 - \omega_1) \\ & = g_\eta + \mathbb{E}_{\tau, \epsilon}[\tilde{\mu}(\omega_1)h(\omega_1) + \tilde{\mu}^*(\omega_2)h(\omega_2) \\ & + \tilde{\mu}(\omega_2 - \omega_1)h(\omega_2 - \omega_1)] \\ & = g_\eta + \mathbb{E}_{\tau, \epsilon}[R_\sigma]. \end{aligned}$$

\square

After empirical centering by R_σ , we can decompose the computable quantity into two pieces for easier analysis:

$$\frac{1}{M} \sum_{j=1}^M By_j - R_\sigma = \tilde{g}_\eta + \tilde{g}_\sigma,$$

where

$$\tilde{g}_\eta := \frac{1}{M} \sum_{j=1}^M Bf_j, \quad \tilde{g}_\sigma := \frac{1}{M} \sum_{j=1}^M (By_j - Bf_j) - R_\sigma.$$

Such a decomposition will allow us to leverage the results for Model 3 to control \tilde{g}_η . We let $R_j := By_j - Bf_j$ denote the deviation in the definition of \tilde{g}_σ .

Note $\tilde{g}_\eta + \tilde{g}_\sigma$ is not smooth due to the additive noise. Thus to deal with the third challenge, we need to add a smoothing procedure. Let $\phi_L(r) = (2\pi L^2)^{-1/2} e^{-r^2/(2L^2)}$ be a low pass filter. We define a new estimator for Model 2 as

$$\begin{aligned} (\widetilde{Bf})(r, \theta) := & (I - LC_0)^{-1} C_1 LC_2 \\ & [4((\tilde{g}_\eta + \tilde{g}_\sigma) * \phi_L)(r, \theta) + r\partial_r((\tilde{g}_\eta + \tilde{g}_\sigma) * \phi_L)(r, \theta)]. \end{aligned} \quad (7)$$

To bound the MSE of the above estimator, we will use the following four lemmas. Lemmas 3 and 3 generalize Lemmas 2 and 3 in [24]; Lemma 5 generalizes Lemma D.1 in [23]; the proofs of all three are provided in the supplemental material for completeness.

Lemma 3. *Let $q \in L^2(\mathbb{R}^2)$ and assume $|\hat{q}(\omega)|$ decays like $|\omega|^{-\alpha}$ for some integer $\alpha \geq 2$, i.e. there exist*

constants C, ω_0 such that $|\hat{q}(\omega)| \leq C|\omega|^{-\alpha}$ for $|\omega| > \omega_0$. Then for L small enough,

$$\|q - q * \phi_L\|_2^2 \lesssim \|q\|_2^2 L^4 + L^{4\wedge(2\alpha-2)}.$$

Lemma 4. Let $r\hat{q}(r, \theta) \in L^2(\mathbb{R}^2, dr \times d\theta)$ and assume its Fourier transform $\widehat{(\cdot)q(\cdot)}(\omega)$ decays like $|\omega|^{-\alpha}$ for some integer $\alpha \geq 2$. Then for L small enough,

$$\|r(q - q * \phi_L)(r, \theta)\|_2^2 \lesssim \|r\hat{q}(r, \theta)\|_2^2 L^4 + L^{4\wedge(2\alpha-2)} + (L^3 \|q\|_2^2) \wedge (L^4 \|\partial_r q\|_2^2).$$

Lemma 5. Suppose ε is a mean zero Gaussian white noise supported on $[-1/2, 1/2]$ with variance σ^2 . For all $p > 0$ and $\omega \in \mathbb{R}$,

$$\mathbb{E}[|\hat{\varepsilon}(\omega)|^p] \lesssim_p \sigma^p.$$

Lemma 6. Assume that the assumptions of Model 2 hold, $Bf \in C^3(\mathbb{R}^2)$, $(\cdot)\widehat{Bf}(\cdot)$ decays like $|\cdot|^{-\kappa}$ for some $\kappa \geq 3$, and $(Bf)^k \in L^2(\mathbb{R}^2)$ for $k = 2, 3$. Then:

$$\|\tilde{g}_\sigma\|_{L^2(\Omega)}^2 \lesssim_\Omega \frac{\sigma^2}{M} \|f\|_2^4 + \frac{\sigma^4}{M} \|f\|_2^2 + \frac{\sigma^6}{M}.$$

Proof. See Appendix B. \square

We can now bound the error of the bispectrum estimator (7) for the noisy dilation MRA model.

Theorem 3. Assume that the assumptions of Model 2 hold, $Bf \in C^3(\mathbb{R}^2)$, $(\cdot)\widehat{Bf}(\cdot)$ decays like $|\cdot|^{-\kappa}$ for some $\kappa \geq 3$, and $(Bf)^k \in L^2(\mathbb{R}^2)$ for $k = 2, 3$. For the estimator $(\widetilde{Bf})(r, \theta)$ defined in (7),

$$\mathbb{E} \left[\|\widetilde{Bf} - Bf\|_{L^2(\Omega)}^2 \right] \leq C_{f,\Omega} \left(\frac{\eta^2}{M} + L^4 + \frac{\sigma^2 \vee \sigma^6}{L^2 M} \right),$$

where $C_{f,\Omega}$ only depends on f and Ω .

Proof. First, since $(I - L_{C_0})^{-1} C_1 L_{C_2}$ is a bounded linear operator as in Lemma 1,

$$\begin{aligned} & \|Bf - \widetilde{Bf}\|_{L^2(\Omega)}^2 \\ & \lesssim \|g_\eta - \tilde{g}_\eta\|_{L^2(\Omega)}^2 + \|r\partial_r g_\eta - r\partial_r \tilde{g}_\eta\|_{L^2(\Omega)}^2 \\ & + \|\tilde{g}_\eta - \tilde{g}_\eta * \phi_L\|_{L^2(\Omega)}^2 + \|r\partial_r \tilde{g}_\eta - r\partial_r (\tilde{g}_\eta * \phi_L)\|_{L^2(\Omega)}^2 \\ & + \|\tilde{g}_\sigma * \phi_L\|_{L^2(\Omega)}^2 + \|r\partial_r (\tilde{g}_\sigma * \phi_L)\|_{L^2(\Omega)}^2. \end{aligned}$$

By Theorem 2,

$$\begin{aligned} & \mathbb{E} \left[\|g_\eta - \tilde{g}_\eta\|_{L^2(\Omega)}^2 + \|r\partial_r g_\eta - r\partial_r \tilde{g}_\eta\|_{L^2(\Omega)}^2 \right] \\ & \lesssim \frac{\eta^2}{M} \|(Bf)(r, \theta)\|_2^2 + \frac{\eta^2}{M} \|r\partial_r (Bf)(r, \theta)\|_2^2 \\ & + \frac{\eta^2}{M} \|r^2 \partial_{rr} (Bf)(r, \theta)\|_2^2 + O_f \left(\frac{\eta^4}{M} \right). \end{aligned}$$

It remains to bound the other four terms. By Lemma 2,

$$\|\tilde{g}_\eta - \tilde{g}_\eta * \phi_L\|_{L^2(\Omega)}^2 \lesssim \|\tilde{g}_\eta\|_2^2 L^4 + L^{4\wedge(2\kappa-2)}.$$

Since

$$\|Bf_j\|_2^2 = (1 - \tau_j)^4 \|Bf\|_2^2 \leq 2^4 \|Bf\|_2^2,$$

applying triangle inequality yields

$$\|\tilde{g}_\eta\|_2 = \left\| \frac{1}{M} \sum_{j=1}^M Bf_j \right\|_2 \leq \frac{1}{M} \sum_{j=1}^M \|Bf_j\|_2 \lesssim \|Bf\|_2,$$

and we obtain

$$\|\tilde{g}_\eta - \tilde{g}_\eta * \phi_L\|_{L^2(\Omega)} \lesssim \|Bf\|_2^2 L^4 + L^{4\wedge(2\kappa-2)}.$$

Also, by Lemma 4,

$$\begin{aligned} & \|r\partial_r (\tilde{g}_\eta - (\tilde{g}_\eta * \phi_L))\|_{L^2(\Omega)}^2 \\ & \lesssim \|r\partial_r \tilde{g}_\eta\|_2^2 L^4 + L^{4\wedge(2\kappa-2)} + L^4 \|\partial_{rr} \tilde{g}_\eta\|_2^2 \\ & \lesssim (\|r\partial_r (Bf)(r, \theta)\|_2^2 + 1 + \|\partial_{rr} (Bf)(r, \theta)\|_2^2) L^4. \end{aligned}$$

Now consider the additive noise terms. By Young's Convolution Inequality and Lemma 6,

$$\begin{aligned} \|\tilde{g}_\sigma * \phi_L\|_{L^2(\Omega)}^2 & \leq \|\phi_L\|_{L^1(\Omega)}^2 \|\tilde{g}_\sigma\|_{L^2(\Omega)}^2 \\ & \lesssim \|\tilde{g}_\sigma\|_{L^2(\Omega)}^2 \\ & \lesssim_\Omega \frac{\sigma^2}{M} \|f\|_2^4 + \frac{\sigma^4}{M} \|f\|_2^2 + \frac{\sigma^6}{M} \\ & \lesssim_{\Omega, f} \left(\frac{\sigma^2 \vee \sigma^6}{M} \right). \end{aligned}$$

Now we consider $\|r\partial_r (\tilde{g}_\sigma * \phi_L)\|_{L^2(\Omega)}$. Let $R_\Omega = \max_\Omega |r|$. We have

$$\begin{aligned} \|r\partial_r (\tilde{g}_\sigma * \phi_L)\|_{L^2(\Omega)}^2 & \leq R_\Omega^2 \|\tilde{g}_\sigma * \partial_r \phi_L\|_{L^2(\Omega)}^2 \\ & \leq R_\Omega^2 \|\partial_r \phi_L\|_1^2 \|\tilde{g}_\sigma\|_{L^2(\Omega)}^2. \end{aligned}$$

Since ϕ is a radial filter and

$$\partial_r \phi_L(r) = -(2\pi L^3)^{-1/2} r e^{-r^2/(2L^2)},$$

we obtain

$$\|\partial_r \phi_L\|_1 = \frac{1}{L^3} \int_0^\infty r e^{-r^2/(2L^2)} dr = L^{-1}$$

so that $\|\partial_r \phi_L\|_1^2 = L^{-2}$. Combining with the bound for $\|\tilde{g}_\sigma\|_{L^2(\Omega)}^2$, we obtain

$$\|r\partial_r (\tilde{g}_\sigma * \phi_L)\|_{L^2(\Omega)}^2 \lesssim_{\Omega, f} L^{-2} \left(\frac{\sigma^2 \vee \sigma^6}{M} \right).$$

Combining terms finishes the proof. \square

Remark 1. When $\sigma \geq 1$, the upper bound in Theorem 3 is minimized by choosing $L = \frac{\sigma}{M^{1/6}}$, yielding a convergence rate of $O\left(\frac{\eta^2}{M} + \frac{\sigma^4}{M^{2/3}}\right)$ on the squared error.

V. NUMERICAL IMPLEMENTATION OF BISPECTRUM RECOVERY

Theorem 3 establishes that the estimator $\widetilde{B}f$ defined in (7) is an unbiased estimator of Bf and quantifies the rate of convergence. Note the estimator requires applying the operator $(I - L_{C_0})^{-1}C_1L_{C_2}$ to the empirical data term

$$\tilde{d} := 4(\tilde{g}_\eta + \tilde{g}_\sigma) * \phi_L + r(\tilde{g}_\eta + \tilde{g}_\sigma) * \partial_r \phi_L, \quad (8)$$

and one does not have a closed form formula for applying this operator. However, $\widetilde{B}f$ is the unique solution of a quadratic programming problem, namely:

$$\begin{aligned} \widetilde{B}f &= \operatorname{argmin}_{\hat{g}} \mathcal{L}(\hat{g}), \\ \mathcal{L}(\hat{g}) &= \left\| (I - L_{C_0})\hat{g} - C_1L_{C_2}\tilde{d} \right\|_2^2. \end{aligned} \quad (9)$$

It is thus straight-forward to compute $\widetilde{B}f$ by minimizing the convex function $\mathcal{L}(\hat{g})$.

Remark 2. A computation similar to [24] shows the gradient of the loss is

$$\nabla_{\hat{g}} \mathcal{L}(\hat{g}) = 2(I - L_{C_0})^* ((I - L_{C_0})\hat{g} - C_1L_{C_2}\tilde{d}),$$

where the adjoint acts as

$$\begin{aligned} (I - L_{C_0})^* h(\omega_1, \omega_2) \\ = h(\omega_1, \omega_2) - C_0^2 h(C_0^{-1}\omega_1, C_0^{-1}\omega_2). \end{aligned}$$

There is however a caveat to the above: solving (9) requires knowledge of η , since the constants C_i depend on η , and this parameter is generally unknown. We thus first learn η using the algorithm proposed in [24], which simultaneously approximates η and the power spectrum Pf by solving the joint optimization:

$$(\widetilde{P}f, \tilde{\eta}) = \operatorname{argmin}_{\hat{p} \geq 0, \hat{\eta} \geq 0} \mathcal{L}(\hat{p}, \hat{\eta}), \quad (10)$$

where

$$\mathcal{L}(\hat{p}, \hat{\eta}) = \frac{\| (I - L_{C_0(\hat{\eta})})\hat{p} - C_1(\hat{\eta})L_{C_2(\hat{\eta})}\tilde{q} \|_2^2}{\hat{\eta}^2}. \quad (11)$$

Here \tilde{q} is an empirical data term analogous to (8) but computed from the noisy *power spectra*, and the definitions of $C_i(\eta)$ and L_C have been slightly modified to achieve power spectrum recovery (see [24] for exact definitions). We thus conveniently learn the power spectrum in addition to η , as the algorithm we apply in Section VII to recover the hidden signal requires knowledge of both the bispectrum and power spectrum. Unfortunately, unlike (9), the optimization (10) is nonconvex.

Remark 3. The objective function in [24] in fact contains only the numerator of (11), but we found the modified loss (11) yielded more stable recovery of η , since the numerator vanishes whenever $\hat{\eta} = 0$, regardless of \hat{p} .

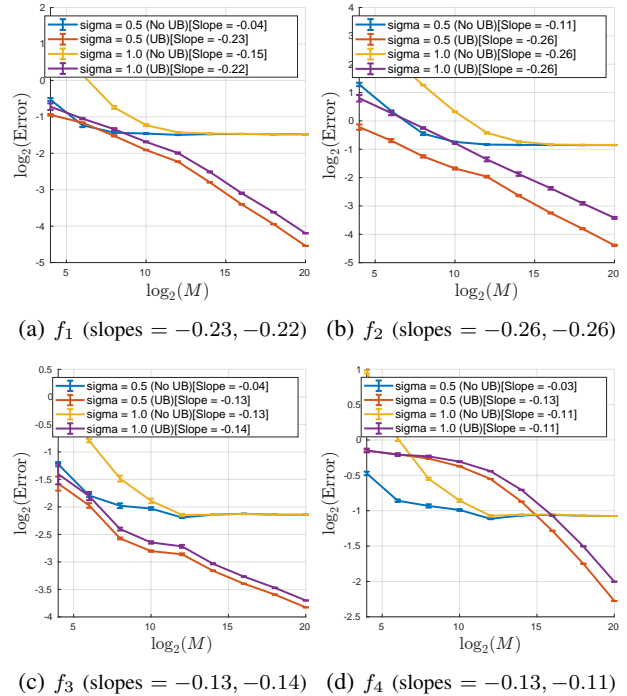


Fig. 2: Bispectrum recovery error with oracle σ, η .

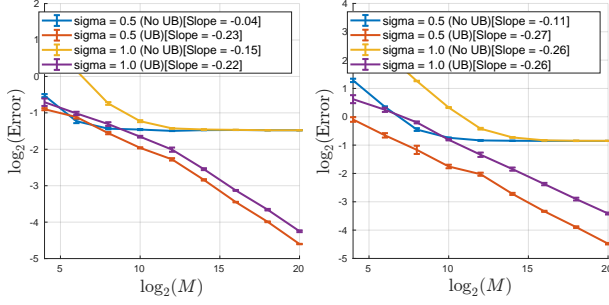
Remark 4. Although the theoretical guarantees of Theorem 3 apply to continuous signals f , in practice we will only observe a discretization of these continuous signals, and the optimization in (9) is not carried out on a function $\hat{g} : \mathbb{R}^2 \rightarrow \mathbb{C}$, but on a matrix $\hat{g}_{i,j} = \hat{g}(\omega_i, \omega_j)$ of discrete frequencies. Thus in addition to the sampling error reported in Theorem 3, we will in practice also be subjected to discretization errors arising from approximating the continuum Fourier transform with the DFT, approximating derivatives using difference quotients, and approximating dilation operators using interpolation. See [24] for a more detailed discussion of these discretization effects.

VI. NUMERICAL EXPERIMENTS FOR BISPECTRUM RECOVERY

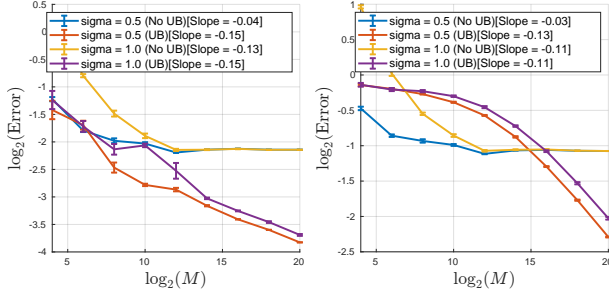
We will now test the accuracy of our bispectrum estimator $\widetilde{B}f$ given in (7) on the following signals:

$$\begin{aligned} f_1(x) &= A_1 e^{-5x^2} \cos(8x) \\ f_2(x) &= A_2 e^{-5x^2} \cos(12x) \\ f_3(x) &= A_3 \operatorname{sinc}(4x) \\ f_4(x) &= A_4 \cos(6x) \mathbf{1}_{\{x \in (-\frac{\pi}{4}, \frac{\pi}{4})\}}. \end{aligned}$$

Like in [23], we define our hidden signals on $[-N/4, N/4]$ and the noisy signals on $[-N/2, N/2]$, and then sample them at a rate of $2^{-\ell}$, choosing $N = 2^5$ and $\ell = 4$. In frequency, the signals were sampled on the interval $[-2^\ell \pi, 2^\ell \pi]$ with sampling rate of π/N .



(a) f_1 (slopes = $-0.23, -0.22$) (b) f_2 (slopes = $-0.27, -0.26$)



(c) f_3 (slopes = $-0.15, -0.15$) (d) f_4 (slopes = $-0.13, -0.11$)

Fig. 3: Bispectrum recovery error with unknown σ, η .

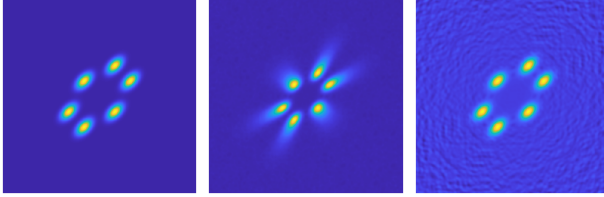
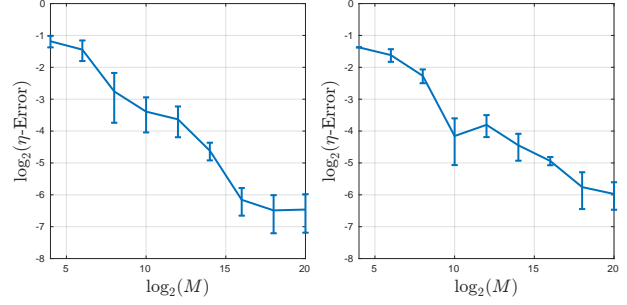


Fig. 4: Example of bispectrum recovery for f_2 with $\eta = 12^{-1/2}$ and $\sigma = 1.0$. **Left:** ground truth signal. **Middle:** average of bispectra after additive noise unbiasing. **Right:** recovered bispectrum using unbiasing procedure.

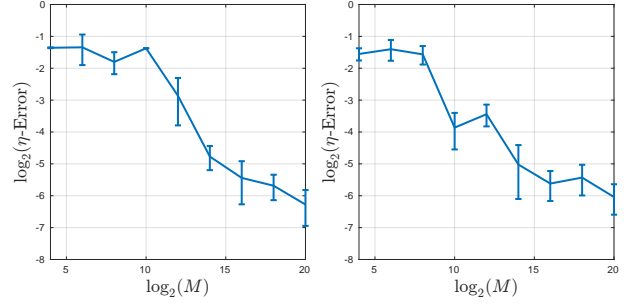
The constants A_i with $i = 1, \dots, 4$ were chosen so that the SNR for each f_i was set to be σ^{-2} , where $\text{SNR} = \left(\int_{-N/2}^{N/2} |f(x)|^2 dx \right) / \sigma^2$. Signals were randomly translated and randomly dilated with τ uniform on $[-\frac{1}{2}, \frac{1}{2}]$, so that the dilation factor $(1 - \tau) \in [\frac{1}{2}, 2]$ and $\eta^2 = \frac{1}{12}$. Signals were then corrupted by Gaussian noise at two different noise levels: $\sigma = 0.5$ and $\sigma = 1$.

These signals were chosen to test the robustness of our proposed method. The signals f_1 and f_2 are smooth with exponential decay in both space and frequency, and thus the proposed method is expected to work well. On the other hand, f_3 is smooth in space, but discontinuous in frequency, so in this example the assumption of a smooth bispectrum is violated. Also, f_4 is continuous but not smooth in space, and thus poses a challenge due to its slowly decaying FT.

We start with the case where σ and η are given



(a) f_1 (b) f_2



(c) f_3 (d) f_4

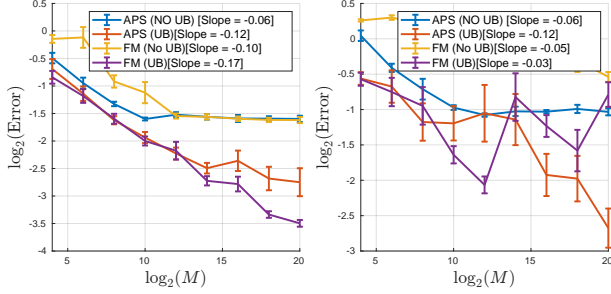
Fig. 5: η estimation plots with standard error bars.

by an oracle. Figure 2 shows the relative L^2 error of bispectrum recovery, i.e. $\text{Error} = \|Bf - \hat{B}f\|_2 / \|Bf\|_2$, as the sample size M is increased. NO UB is an average of the noisy bispectra with an empirical centering to account for the bias from additive noise, and UB is with our unbiasing procedure. Figure 4 illustrates how the proposed unbiasing procedure is able to remove the effect of the dilations for a fixed signal (f_2) and sample size. All experiments were run with a Gaussian width of $L = 5\sigma M^{-1/6}$ (see Remark 1). Note based on Remark 1, we expect to see the error decay approximately like $O(M^{-1/3})$, i.e. we expect to observe a slope of $-1/3$ on a log-log plot. For f_1 and f_2 , the error decay is close to the theoretical bound (observed slope around $-1/4$). For f_3 and f_4 where some Model assumptions are violated, the decay is slower but still consistently linear, which yields empirical evidence that $\hat{B}f$ is still an unbiased estimator of Bf .

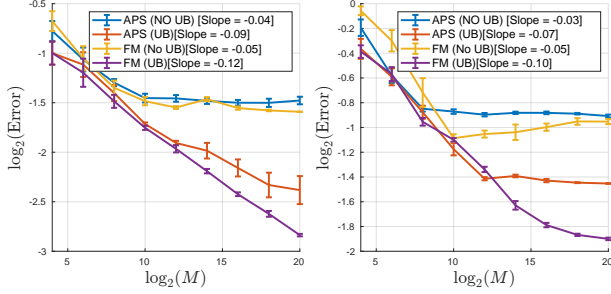
We next investigate bispectrum recovery when σ and η are unknown. Note when \hat{f} has a fast decay, σ can be accurately estimated from the decay of the power spectrum, i.e. by

$$\tilde{\sigma}^2 := \frac{1}{|\{\omega_i \in \Sigma\}|} \sum_{\omega_i \in \Sigma} |\hat{y}(\omega_i)|^2,$$

where $\Sigma = [-2^\ell \pi, 2^\ell \pi] \setminus [-2^{\ell-1} \pi, 2^{\ell-1} \pi]$. Estimating η is more difficult but can be accomplished via a joint optimization as described in Section V. Figure 5 shows



(a) f_1 (slopes = $-0.12, -0.17$) (b) f_2 (slopes = $-0.12, -0.03$)



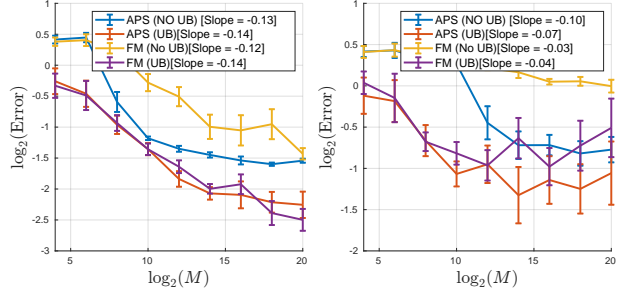
(c) f_3 (slopes = $-0.09, -0.12$) (d) f_4 (slopes = $-0.07, -0.10$)

Fig. 6: Hidden signal recovery error plots with oracle $\eta = 12^{-1/2}$ and $\sigma = 0.5$. First reported slope is for UB with APS, and second is UB with FM.

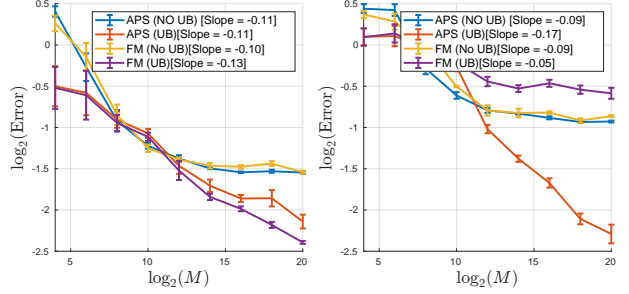
the error for η recovery, and we see that η can be learned reliably for large M . Figure 3 shows the bispectrum recovery error when η, σ are empirically estimated, and the results are nearly identical to the oracle case given in Figure 2, indicating that accurate bispectrum estimation is still possible.

VII. HIDDEN SIGNAL RECOVERY

Once the bispectrum of the hidden signal is recovered, a bispectrum inversion algorithm must be applied to recover the hidden signal. Jennrich's algorithm provides a stability guarantee for this inversion [38], [22], [28], but is not suitable for practical applications. Other approaches include non-convex optimization over the manifold of phases [6], iterative phase synchronization [6], semi-definite programming, phase unwrapping, frequency marching [20], [41], and the spectral method proposed in [11]. We refer the reader to [6] for a survey and comparison of algorithms. Although we do not rigorously analyze inversion in this article, we nonetheless investigate empirically whether the bispectra recovered in Section VI can be accurately inverted to recover the hidden signal, i.e. whether the proposed method can fully solve the MRA problem. We invert our recovered bispectra using iterative phase synchronization (APS) and frequency marching (FM) (see [6]); note the inversion also requires knowledge of the power spectrum, which



(a) f_1 (slopes = $-0.14, -0.14$) (b) f_2 (slopes = $-0.07, -0.04$)



(c) f_3 (slopes = $-0.11, -0.13$) (d) f_4 (slopes = $-0.17, -0.05$)

Fig. 7: Hidden signal recovery error plot with unknown $\eta = 12^{-1/2}$ and $\sigma = 1.0$. First reported slope is for UB with APS, and second is UB with FM.

we learn using [24] as described in Section V. The resulting L^2 relative error of hidden signal recovery for the oracle and empirical cases are given in Figures 6 and 7 respectively. Note that the estimated signal \tilde{f} is only defined up to translation, and the error is thus computed by $\min_t \|f(x) - \tilde{f}(x-t)\|_2 / \|f\|_2$. For brevity we only report the easiest case ($\sigma = 0.5$, oracle) and the hardest case ($\sigma = 1$, empirical). Although FM outperformed APS on the low frequency signals in the low noise regime, we found APS to be more reliable across a range of signals and noise levels (for example, FM performs poorly on the medium frequency Gabor f_2 ; see Figure 6). In general we observe that the hidden signal can be accurately estimated for large values of M , but the inversion process unfortunately increases the error, i.e. for large M the hidden signal recovery error is typically 3-4 times larger than the bispectrum recovery error, and generally more variable.

To complement our quantitative error plots, we also provide a qualitative assessment. In Figures 8 and 9, examples of the output are provided using $M = 2^{20}$ samples (red curves), and we compare with the output if dilation unbiasing were not applied (blue curves). Our recovered signals capture well the general shape of the ground truth signals, and generally decrease the relative error of the hidden signal recovery by a factor of 2-4 (except for f_3 in the high noise regime). On the

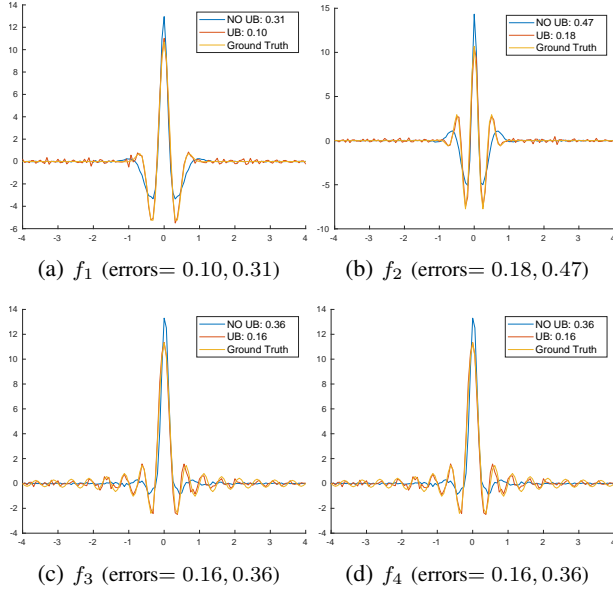


Fig. 8: Hidden signal recovery with oracle $\eta = 12^{-1/2}$ and $\sigma = 0.5$. First reported error is for UB; second reported error is for NO UB.

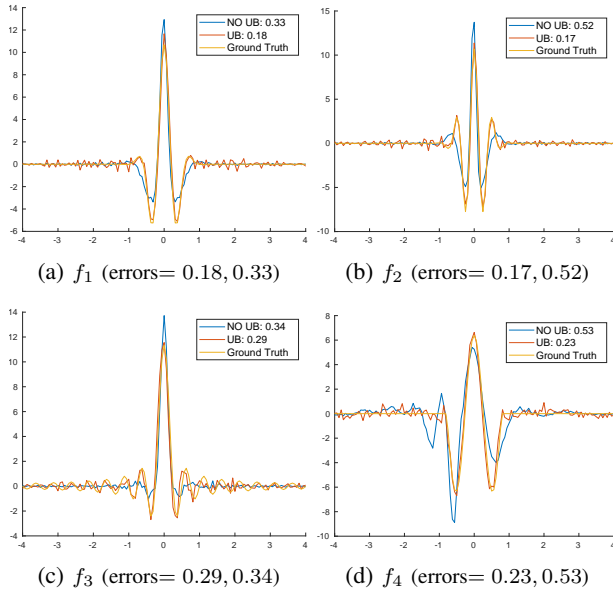


Fig. 9: Hidden signal recovery plots with unknown $\eta = 12^{-1/2}$ and $\sigma = 1.0$. First reported error is for UB; second reported error is for NO UB.

other hand, without our unbiasing procedure, the output contains bias from the dilations, and the general shape of the recovered signals is incorrect, with the recovered peaks out of alignment.

VIII. CONCLUSION

We study the MRA problem under the action of the non-compact dilation group, in addition to translation and additive noise. We present a novel technique for removing the dilation bias from the bispectrum, so that when the method is combined with bispectrum inversion it fully solves this MRA model. Since in many applications the assumption of a uniform distribution may fail, an important future direction is investigating whether the dilation distribution can be learned empirically and, if so, extending the method to an arbitrary but known dilation distribution. Also of interest is extending the method to higher dimensional signals, which is straightforward for Model 2, although computationally more burdensome. In higher dimensions however it is natural to incorporate rotations into the model, which poses additional challenges, as the rotation group in \mathbb{R}^3 is not commutative.

REFERENCES

- [1] Emmanuel Abbe, Tamir Bendory, William Leeb, João M Pereira, Nir Sharon, and Amit Singer. Multireference alignment is easier with an aperiodic translation distribution. *IEEE Transactions on Information Theory*, 65(6):3565–3584, 2018.
- [2] Afonso Bandeira, Yutong Chen, Roy R Lederman, and Amit Singer. Non-unique games over compact groups and orientation estimation in cryo-em. *Inverse Problems*, 2020.
- [3] Afonso S Bandeira, Ben Blum-Smith, Joe Kileel, Amelia Perry, Jonathan Weed, and Alexander S Wein. Estimation under group actions: recovering orbits from invariants. *arXiv preprint arXiv:1712.10163*, 2017.
- [4] Afonso S Bandeira, Nicolas Boumal, and Vladislav Voroninski. On the low-rank approach for semidefinite programs arising in synchronization and community detection. In *Conference on learning theory*, pages 361–382, 2016.
- [5] Afonso S Bandeira, Moses Charikar, Amit Singer, and Andy Zhu. Multireference alignment using semidefinite programming. In *Proceedings of the 5th conference on Innovations in theoretical computer science*, pages 459–470. ACM, 2014.
- [6] Tamir Bendory, Nicolas Boumal, Chao Ma, Zhizhen Zhao, and Amit Singer. Bispectrum inversion with application to multireference alignment. *IEEE Transactions on Signal Processing*, 66(4):1037–1050, 2017.
- [7] Nicolas Boumal. Nonconvex phase synchronization. *SIAM Journal on Optimization*, 26(4):2355–2377, 2016.
- [8] Lisa Gottesfeld Brown. A survey of image registration techniques. *ACM computing surveys (CSUR)*, 24(4):325–376, 1992.
- [9] L Capodiferro, R Cusani, G Jacovitti, and M Vascotto. A correlation based technique for shift, scale, and rotation independent object identification. In *ICASSP'87: IEEE International Conference on Acoustics, Speech, and Signal Processing*, volume 12, pages 221–224. IEEE, 1987.
- [10] Vinod Chandran and Stephen L Elgar. Position, rotation, and scale invariant recognition of images using higher-order spectra. In *ICASSP'92: IEEE International Conference on Acoustics, Speech, and Signal Processing*, volume 5, pages 213–216. IEEE, 1992.
- [11] Hua Chen, Mona Zehni, and Zhizhen Zhao. A spectral method for stable bispectrum inversion with application to multireference alignment. *IEEE Signal Processing Letters*, 25(7):911–915, 2018.
- [12] Yuxin Chen and Emmanuel J Candès. The projected power method: An efficient algorithm for joint alignment from pairwise differences. *Communications on Pure and Applied Mathematics*, 71(8):1648–1714, 2018.

- [13] Yuxin Chen, Leonidas J Guibas, and Qi-Xing Huang. Near-optimal joint object matching via convex relaxation. In *Proceedings of the 31st International Conference on Machine Learning*, volume 32 of *Proceedings of Machine Learning Research*, pages 100–108, 2014.
- [14] WB Collis, PR White, and JK Hammond. Higher-order spectra: the bispectrum and trispectrum. *Mechanical systems and signal processing*, 12(3):375–394, 1998.
- [15] Arthur P Dempster, Nan M Laird, and Donald B Rubin. Maximum likelihood from incomplete data via the em algorithm. *Journal of the Royal Statistical Society: Series B (Methodological)*, 39(1):1–22, 1977.
- [16] Robert Diamond. On the multiple simultaneous superposition of molecular structures by rigid body transformations. *Protein Science*, 1(10):1279–1287, 1992.
- [17] Diana Ekman, Åsa K Björklund, Johannes Frey-Skött, and Arne Elofsson. Multi-domain proteins in the three kingdoms of life: orphan domains and other unassigned regions. *Journal of molecular biology*, 348(1):231–243, 2005.
- [18] Federico Forneris, Jin Wu, and Piet Gros. The modular serine proteases of the complement cascade. *Current opinion in structural biology*, 22(3):333–341, 2012.
- [19] Hassan Foroosh, Josiane B Zerubia, and Marc Berthod. Extension of phase correlation to subpixel registration. *IEEE transactions on image processing*, 11(3):188–200, 2002.
- [20] Georgios B Giannakis. Signal reconstruction from multiple correlations: frequency-and time-domain approaches. *JOSA A*, 6(5):682–697, 1989.
- [21] Lars Peter Hansen. Large sample properties of generalized method of moments estimators. *Econometrica: Journal of the Econometric Society*, pages 1029–1054, 1982.
- [22] Richard A Harshman et al. Foundations of the parafac procedure: Models and conditions for an “explanatory” multimodal factor analysis. 1970.
- [23] Matthew Hirn and Anna Little. Wavelet invariants for statistically robust multi-reference alignment. *Information and Inference: A Journal of the IMA*, 10(4):1287–1351, 2021.
- [24] Matthew Hirn and Anna Little. Power spectrum unbiasing for dilation-invariant multi-reference alignment. *Journal of Fourier Analysis and Applications*, 29(4):43, 2023.
- [25] Kazuhiro Hotta, Taketoshi Mishima, and Takio Kurita. Scale invariant face detection and classification method using shift invariant features extracted from log-polar image. *IEICE Transactions on Information and Systems*, 84(7):867–878, 2001.
- [26] Zvi Kam. The reconstruction of structure from electron micrographs of randomly oriented particles. In *Electron Microscopy at Molecular Dimensions*, pages 270–277. Springer, 1980.
- [27] Fima C Klebaner. *Introduction to stochastic calculus with applications*. World Scientific Publishing Company, 2012.
- [28] Sue E Leurgans, Robert T Ross, and Rebecca B Abel. A decomposition for three-way arrays. *SIAM Journal on Matrix Analysis and Applications*, 14(4):1064–1083, 1993.
- [29] Michael Levitt. Nature of the protein universe. *Proceedings of the National Academy of Sciences*, 106(27):11079–11084, 2009.
- [30] Wendell A Lim. The modular logic of signaling proteins: building allosteric switches from simple binding domains. *Current opinion in structural biology*, 12(1):61–68, 2002.
- [31] Stéphane Mallat. Group invariant scattering. *Communications on Pure and Applied Mathematics*, 65(10):1331–1398, October 2012.
- [32] Daniel Martinec and Tomas Pajdla. Robust rotation and translation estimation in multiview reconstruction. In *2007 IEEE Conference on Computer Vision and Pattern Recognition*, pages 1–8. IEEE, 2007.
- [33] Adrien Meynard and Bruno Torrèsani. Spectral analysis for nonstationary audio. *IEEE/ACM Transactions on Audio, Speech, and Language Processing*, 26(12):2371–2380, 2018.
- [34] Harold Omer and Bruno Torrèsani. Estimation of frequency modulations on wideband signals; applications to audio signal analysis. *arXiv preprint arXiv:1305.3095*, 2013.
- [35] Harold Omer and Bruno Torrèsani. Time-frequency and time-scale analysis of deformed stationary processes, with application to non-stationary sound modeling. *Applied and Computational Harmonic Analysis*, 43(1):1–22, 2017.
- [36] Wooram Park and Gregory S Chirikjian. An assembly automation approach to alignment of noncircular projections in electron microscopy. *IEEE Transactions on Automation Science and Engineering*, 11(3):668–679, 2014.
- [37] Wooram Park, Charles R Midgett, Dean R Madden, and Gregory S Chirikjian. A stochastic kinematic model of class averaging in single-particle electron microscopy. *The International journal of robotics research*, 30(6):730–754, 2011.
- [38] Amelia Perry, Jonathan Weed, Afonso Bandeira, Philippe Rigollet, and Amit Singer. The sample complexity of multi-reference alignment. *SIAM Journal on Mathematics of Data Science*, 1(3):497–517, 2019.
- [39] Nir Sharon, Alexander S Wein, Afonso S Bandeira, and Ankur Moitra. Message-passing algorithms for synchronization problems over compact groups. *Communications on Pure and Applied Mathematics*, 71(11):2275–2322, 2018.
- [40] Dirk Robinson, Sina Farsiu, and Peyman Milanfar. Optimal registration of aliased images using variable projection with applications to super-resolution. *The Computer Journal*, 52(1):31–42, 2007.
- [41] Brian M Sadler and Georgios B Giannakis. Shift-and rotation-invariant object reconstruction using the bispectrum. *JOSA A*, 9(1):57–69, 1992.
- [42] Sjors HW Scheres, Mikel Valle, Rafael Nuñez, Carlos OS Sorzano, Roberto Marabini, Gabor T Herman, and Jose-Maria Carazo. Maximum-likelihood multi-reference refinement for electron microscopy images. *Journal of molecular biology*, 348(1):139–149, 2005.
- [43] Nir Sharon, Joe Kileel, Yuehaw Khoo, Boris Landa, and Amit Singer. Method of moments for 3-D single particle ab initio modeling with non-uniform distribution of viewing angles. *Inverse Problems*, 36(4):044003, 2020.
- [44] Amit Singer. Angular synchronization by eigenvectors and semidefinite programming. *Applied and computational harmonic analysis*, 30(1):20–36, 2011.
- [45] Douglas L Theobald and Phillip A Steindel. Optimal simultaneous superpositioning of multiple structures with missing data. *Bioinformatics*, 28(15):1972–1979, 2012.
- [46] Michail K Tsatsanis and Georgios B Giannakis. Translation, rotation, and scaling invariant object and texture classification using polyspectra. In *Advanced Signal Processing Algorithms, Architectures, and Implementations*, volume 1348, pages 103–115. International Society for Optics and Photonics, 1990.
- [47] Yiqiao Zhong and Nicolas Boumal. Near-optimal bounds for phase synchronization. *SIAM Journal on Optimization*, 28(2):989–1016, 2018.
- [48] J Portegies Zwart, René van der Heiden, Sjoerd Gelsema, and Frans Groen. Fast translation invariant classification of hrr range profiles in a zero phase representation. *IEE Proceedings-Radar, Sonar and Navigation*, 150(6):411–418, 2003.

APPENDIX

A. Proof of Theorem 2

First, assume that the $Bf : \mathbb{R}^2 \rightarrow \mathbb{R}$. The argument will be generalized to the complex case after. Notice that

$$|\tilde{g}_\eta(r, \theta) - g_\eta(r, \theta)|^2 = \left| \frac{1}{M} \sum_{j=1}^M (Bf_j)(r, \theta) - g_\eta(r, \theta) \right|^2.$$

Define

$$X_j = Bf_j(r, \theta) - g_\eta(r, \theta) = Bf_j(r, \theta) - \mathbb{E}[(Bf_j)(r, \theta)].$$

This means each X_j is zero centered, so we have

$$\mathbb{E} \left[\left| \frac{1}{M} \sum_{j=1}^M X_j \right|^2 \right] = \text{var} \left[\frac{1}{M} \sum_{j=1}^M X_j \right] = \frac{\text{var}(X_j)}{M}.$$

Write

$$X_j = Bf_j(r, \theta) - (Bf)(r, \theta) + (Bf)(r, \theta) - \mathbb{E}[(Bf_j)(r, \theta)].$$

Then

$$X_j^2 \lesssim (Bf_j(r, \theta) - (Bf)(r, \theta))^2 + ((Bf)(r, \theta) - \mathbb{E}[(Bf_j)(r, \theta)])^2.$$

and

$$\begin{aligned} \mathbb{E}[X_j^2] &\lesssim \mathbb{E}[(Bf_j(r, \theta) - (Bf)(r, \theta))^2] \\ &\quad + \mathbb{E}[(Bf)(r, \theta) - \mathbb{E}[(Bf_j)(r, \theta)]]^2 \\ &\lesssim \mathbb{E}[(Bf_j(r, \theta) - (Bf)(r, \theta))^2]. \end{aligned}$$

Each τ_j has bounded variance and is supported on $[-1/2, 1/2]$. Taylor expand the dilated bispectrum in radial variable in interval $[r/2, 2r]$:

$$\begin{aligned} (Bf)((1 - \tau_j)r, \theta) &= (Bf)(r, \theta) - \partial_r(Bf)(r, \theta)r\tau_j \\ &\quad + \frac{1}{2}\partial_{rr}(Bf)(r, \theta)\Big|_{r=\alpha} r^2\tau_j^2, \end{aligned}$$

with $\alpha \in [r/2, 2r]$. Now multiply both sides by $(1 - \tau_j)^3$ to get

$$\begin{aligned} (Bf_j)(r, \theta) &= (1 - \tau_j)^3(Bf)((1 - \tau_j)r, \theta) \\ &= (1 - \tau_j)^3(Bf)(r, \theta) \\ &\quad - (1 - \tau_j)^3\partial_r(Bf)(r, \theta)r\tau_j \\ &\quad + (1 - \tau_j)^3\frac{1}{2}\partial_{\alpha\alpha}(Bf)(\alpha, \theta)r^2\tau_j^2. \end{aligned}$$

with $\alpha \in [r/2, 2r]$. It now follows that

$$\begin{aligned} (Bf_j)(r, \theta) - (Bf)(r, \theta) &= (3\tau_j^2 - 3\tau_j - \tau_j^3)(Bf)(r, \theta) \\ &\quad - (1 - \tau_j)^3\partial_r(Bf)(r, \theta)r\tau_j \\ &\quad + \frac{1}{2}(1 - \tau_j)^3\partial_{\alpha\alpha}(Bf)(\alpha, \theta)r^2\tau_j^2. \end{aligned}$$

with $\alpha \in [r/2, 2r]$.

Square both sides to get:

$$\begin{aligned} ((Bf_j)(r, \theta) - (Bf)(r, \theta))^2 &= (3\tau_j^2 - \tau_j - \tau_j^3)^2(Bf)^2(r, \theta) \\ &\quad - 2(3\tau_j^2 - \tau_j - \tau_j^3)(1 - \tau_j)^3(Bf)(r, \theta)\partial_r(Bf)(r, \theta)r\tau_j \\ &\quad + (3\tau_j^2 - \tau_j - \tau_j^3)(1 - \tau_j)^3(Bf)(r, \theta)\partial_{\alpha\alpha}(Bf)(\alpha, \theta)r^2\tau_j^2 \\ &\quad + (1 - \tau_j)^6[\partial_r(Bf)(r, \theta)]^2r^2\tau_j^2 \\ &\quad - (1 - \tau_j)^6\partial_r(Bf)(r, \theta)\partial_{\alpha\alpha}(Bf)(\alpha, \theta)r^3\tau_j^3 \\ &\quad + \frac{(1 - \tau_j)^6}{4}[\partial_{\alpha\alpha}(Bf)(\alpha, \theta)]^2r^4\tau_j^4. \end{aligned}$$

Using the inequality $2|ab| \leq |a|^2 + |b|^2$, it follows that

$$\begin{aligned} &2|(\tau_j^2 - \tau_j - \tau_j^3)(1 - \tau_j)^3(Bf)(r, \theta)\partial_r(Bf)(r, \theta)r\tau_j| \\ &\leq (\tau_j^2 - \tau_j - \tau_j^3)^2|(Bf)(r, \theta)|^2 \\ &\quad + (1 - \tau_j)^6|\partial_r(Bf)(r, \theta)r\tau_j|^2 \end{aligned}$$

and

$$\begin{aligned} &|(3\tau_j^2 - \tau_j - \tau_j^3)(1 - \tau_j)^3(Bf)(r, \theta)\partial_{\alpha\alpha}(Bf)(\alpha, \theta)r^2\tau_j^2| \\ &\leq \frac{1}{2}(3\tau_j^2 - \tau_j - \tau_j^3)^2|(Bf)(r, \theta)|^2 \\ &\quad + \frac{1}{2}|1 - \tau_j|^6|\partial_{\alpha\alpha}(Bf)(\alpha, \theta)r^2\tau_j^2|^2. \end{aligned}$$

and

$$\begin{aligned} &|(1 - \tau_j)^6\partial_r(Bf)(r, \theta)\partial_{\alpha\alpha}(Bf)(\alpha, \theta)r^3\tau_j^3| \\ &\leq \frac{1}{2}(1 - \tau_j)^6|\partial_r(Bf)(r, \theta)\tau_jr|^2 \\ &\quad + \frac{1}{2}|1 - \tau_j|^6|\partial_{\alpha\alpha}(Bf)(\alpha, \theta)r^2\tau_j^2|^2. \end{aligned}$$

Take the expectation of both sides now. Since the pdf of τ is supported on $[-1/2, 1/2]$ and zero centered,

$$\mathbb{E}[(3\tau_j^2 - \tau_j - \tau_j^3)^2] \lesssim \mathbb{E}[\tau_j^2] \lesssim \eta^2.$$

The other terms with τ_j are bounded in a similar way. Thus

$$\begin{aligned} &\mathbb{E}[(Bf_j)(r, \theta) - (Bf)(r, \theta)]^2 \\ &\lesssim \eta^2(Bf)^2(r, \theta) + r^2\eta^2[\partial_r(Bf)(r, \theta)]^2 \\ &\quad + \eta^4r^4 \left[\max_{\alpha \in [r/2, 2r]} |\partial_{\alpha\alpha}(Bf)(\alpha, \theta)| \right]^2. \end{aligned}$$

We also have

$$\begin{aligned} \text{var}[X_j] &= \mathbb{E}[X_j^2] \\ &\lesssim \mathbb{E}[(Bf_j)(r, \theta) - (Bf)(r, \theta)]^2 \\ &\lesssim \eta^2(Bf)^2(r, \theta) + r^2\eta^2[\partial_r(Bf)(r, \theta)]^2 \\ &\quad + \eta^4r^4 \left[\max_{\alpha \in [r/2, 2r]} |\partial_{\alpha\alpha}(Bf)(\alpha, \theta)| \right]^2, \end{aligned}$$

and

$$\begin{aligned} &\mathbb{E}[(g_\eta(r, \theta) - \tilde{g}_\eta(r, \theta))^2] \\ &\lesssim \frac{\eta^2}{M}(Bf)^2(r, \theta) + r^2\frac{\eta^2}{M}[\partial_r(Bf)(r, \theta)]^2 \\ &\quad + \frac{\eta^4}{M}r^4 \left[\max_{\alpha \in [r/2, 2r]} |\partial_{\alpha\alpha}(Bf)(\alpha, \theta)| \right]^2. \end{aligned}$$

Now we can take the integral and expectation to get

$$\begin{aligned} &\mathbb{E}[\|g_\eta(r, \theta) - \tilde{g}_\eta(r, \theta)\|_2^2] \\ &\lesssim \frac{\eta^2}{M}\|(Bf)(r, \theta)\|_2^2 + \frac{\eta^2}{M}\|r\partial_r(Bf)(r, \theta)\|_2^2 \\ &\quad + \frac{\eta^4}{M}\left\| r^2 \max_{\alpha \in [r/2, 2r]} |\partial_{\alpha\alpha}(Bf)(\alpha, \theta)| \right\|_2^2 \end{aligned}$$

The first term is now handled appropriately. We can now repeat a nearly identical argument for the second term. Let $g_j = Bf_j$ and

$$Z_j = r \frac{\partial \tilde{g}_j}{\partial r}(r, \theta) - r \frac{\partial g_j}{\partial r}(r, \theta).$$

We have

$$r \frac{\partial \tilde{g}_j}{\partial r}(r, \theta) - r \frac{\partial g_j}{\partial r}(r, \theta) = \frac{1}{M} \sum_{j=1}^M r \frac{\partial g_j}{\partial r}(r, \theta) - r \frac{\partial g_j}{\partial r}(r, \theta).$$

By Leibniz Rule, we can take the derivative inside the expectation to get $\mathbb{E}[Z_j] = 0$, and a similar argument from before yields

$$Z_j^2 \lesssim \left[r \frac{\partial g_j}{\partial r}(r, \theta) - r \frac{\partial g}{\partial r}(r, \theta) \right]^2 + \left[r \frac{\partial g}{\partial r}(r, \theta) - r \frac{\partial g_j}{\partial r}(r, \theta) \right]^2$$

and

$$\mathbb{E}[Z_j^2] \lesssim \mathbb{E} \left[\left(r \frac{\partial g_j}{\partial r}(r, \theta) - r \frac{\partial g}{\partial r}(r, \theta) \right)^2 \right].$$

Taylor expand $\partial_r(Bf)((1 - \tau_j)r, \theta)$ to get

$$\begin{aligned} \partial_r(Bf)((1 - \tau_j)r, \theta) &= \partial_r(Bf)(r, \theta) - \partial_{rr}(Bf)(r, \theta)r\tau_j \\ &\quad + \frac{1}{2}\partial_{\gamma\gamma\gamma}(Bf)(\gamma, \theta)r^2\tau_j^2, \end{aligned}$$

with $\gamma \in [r/2, 2r]$. Since $r \frac{\partial g_j}{\partial r}(r, \theta) = r(1 - \tau_j)^4 \partial_r(Bf)((1 - \tau_j)r, \theta)$, multiply both sides by $(1 - \tau_j)^4$:

$$\begin{aligned} &(1 - \tau_j)^4 r \partial_r(Bf)((1 - \tau_j)r, \theta) \\ &= (1 - \tau_j)^4 r \partial_r(Bf)(r, \theta) \\ &\quad - (1 - \tau_j)^4 \partial_{rr}(Bf)(r, \theta)r^2\tau_j \\ &\quad + (1 - \tau_j)^4 \frac{1}{2} \partial_{\gamma\gamma\gamma}(Bf)(\gamma, \theta)r^3\tau_j^2 \end{aligned}$$

with $\gamma \in [r/2, 2r]$. Then

$$\begin{aligned} &r \frac{\partial g_j}{\partial r}(r, \theta) - r \frac{\partial g}{\partial r}(r, \theta) \\ &= (\tau_j^4 - 4\tau_j^3 + 6\tau_j^2 - 4\tau_j)r \partial_r(Bf)(r, \theta) \\ &\quad - (1 - \tau_j)^4 \partial_{rr}(Bf)(r, \theta)r^2\tau_j \\ &\quad + (1 - \tau_j)^4 \frac{1}{2} \partial_{\gamma\gamma\gamma}(Bf)(\gamma, \theta)r^3\tau_j^2 \end{aligned}$$

with $\gamma \in [r/2, 2r]$. By a similar process from above,

$$\begin{aligned} &\mathbb{E} \left[\left(r \frac{\partial g_j}{\partial r}(r, \theta) - r \frac{\partial g}{\partial r}(r, \theta) \right)^2 \right] \\ &\lesssim \frac{\eta^2}{M} \|\partial_r(Bf)(r, \theta)\|_2^2 + \frac{\eta^2}{M} \|r^2 \partial_{rr}(Bf)(r, \theta)\|_2^2 \\ &\quad + \frac{\eta^4}{M} \left\| r^3 \max_{\gamma \in [r/2, 2r]} |\partial_{\gamma\gamma\gamma}(Bf)(\gamma, \theta)| \right\|_2^2. \end{aligned}$$

Thus, we get the desired bound in the real case. For the case where $Bf : \mathbb{R}^2 \rightarrow \mathbb{C}$, simply write $Bf = \text{Re}(Bf) + i\text{Im}(Bf)$ and repeat the argument above on the real and imaginary parts and add the two norms together.

B. Proof of Lemma 6

We use triangle inequality to get

$$\begin{aligned} &\|\tilde{g}_\sigma\|_{L^2(\Omega)}^2 \\ &\lesssim \left\| \frac{1}{M} \sum_{j=1}^M \hat{f}_j(\omega_1) \hat{f}_j(\omega_2) \hat{\varepsilon}_j(\omega_2 - \omega_1) \right\|_{L^2(\Omega)}^2 \\ &\quad + \left\| \frac{1}{M} \sum_{j=1}^M \hat{f}_j^*(\omega_2) \hat{f}_j(\omega_2 - \omega_1) \hat{\varepsilon}_j(\omega_1) \right\|_{L^2(\Omega)}^2 \\ &\quad + \left\| \frac{1}{M} \sum_{j=1}^M \hat{f}_j(\omega_1) \hat{f}_j(\omega_2 - \omega_1) \hat{\varepsilon}_j^*(\omega_2) \right\|_{L^2(\Omega)}^2 \\ &\quad + \left\| \frac{1}{M} \sum_{j=1}^M B\varepsilon_j(\omega_1, \omega_2) \right\|_{L^2(\Omega)}^2 \\ &\quad + \|B_1\|_{L^2(\Omega)}^2 + \|B_2\|_{L^2(\Omega)}^2 + \|B_3\|_{L^2(\Omega)}^2. \end{aligned}$$

where

$$\begin{aligned} B_1 &= \frac{1}{M} \sum_{j=1}^M \hat{f}_j(\omega_1) \hat{\varepsilon}_j^*(\omega_2) \hat{\varepsilon}_j(\omega_2 - \omega_1) \\ &\quad - h(\omega_1) \tilde{\mu}(\omega_1) \\ B_2 &= \frac{1}{M} \sum_{j=1}^M \hat{f}_j^*(\omega_2) \hat{\varepsilon}_j(\omega_1) \hat{\varepsilon}_j(\omega_2 - \omega_1) \\ &\quad - h(\omega_2) \tilde{\mu}^*(\omega_2) \\ B_3 &= \frac{1}{M} \sum_{j=1}^M \hat{f}_j(\omega_2 - \omega_1) \hat{\varepsilon}_j(\omega_1) \hat{\varepsilon}_j^*(\omega_2) \\ &\quad - h(\omega_2 - \omega_1) \tilde{\mu}(\omega_2 - \omega_1) \end{aligned}$$

and we proceed to bound the expectation of each term. For the first term, we obtain:

$$\begin{aligned} &\mathbb{E} \left[\left\| \frac{1}{M} \sum_{j=1}^M \hat{f}_j(\omega_1) \hat{f}_j^*(\omega_2) \hat{\varepsilon}_j(\omega_2 - \omega_1) \right\|_{L^2(\Omega)}^2 \right] \\ &= \int_{\Omega} \mathbb{E} \left[\left| \frac{1}{M^2} \sum_{j=1}^M \hat{f}_j(\omega_1) \hat{f}_j(\omega_2) \hat{\varepsilon}_j(\omega_2 - \omega_1) \right|^2 \right] d\omega_1 d\omega_2 \\ &= \frac{\sigma^2}{M^2} \int_{\Omega} \sum_{j=1}^M |\hat{f}_j(\omega_1) \hat{f}_j(\omega_2)|^2 d\omega_1 d\omega_2 \\ &= \frac{\sigma^2}{M^2} \sum_{j=1}^M \int_{\Omega} |\hat{f}_j(\omega_1)|^2 d\omega_1 \int_{\Omega} |\hat{f}_j(\omega_2)|^2 d\omega_2 \\ &= \frac{\sigma^2}{M} \|\hat{f}\|_{L^2(\Omega)}^4 \leq \frac{\sigma^2}{M} (2\pi)^2 \|f\|_{L^2(\mathbb{R})}^4. \end{aligned}$$

An identical argument can be applied to bound the second and third terms. For the fourth term, since $\mathbb{E}[B\varepsilon_j] = 0$, we have

$$\begin{aligned} & \mathbb{E} \left[\left\| \frac{1}{M} \sum_{j=1}^M B\varepsilon_j(\omega_1, \omega_2) \right\|_{L^2(\Omega)}^2 \right] \\ &= \mathbb{E} \left[\int_{\Omega} \left| \frac{1}{M} \sum_{j=1}^M B\varepsilon_j(\omega_1, \omega_2) \right|^2 d\omega_1 d\omega_2 \right] \\ &= \int_{\Omega} \mathbb{E} \left[\left| \frac{1}{M} \sum_{j=1}^M B\varepsilon_j(\omega_1, \omega_2) \right|^2 \right] d\omega_1 d\omega_2 \\ &= \int_{\Omega} \text{Var} \left[\frac{1}{M} \sum_{j=1}^M B\varepsilon_j(\omega_1, \omega_2) \right] d\omega_1 d\omega_2 \\ &= \frac{1}{M} \int_{\Omega} \text{Var}(B\varepsilon_j) d\omega_1 d\omega_2. \end{aligned}$$

By Holder's inequality and Lemma 5,

$$\begin{aligned} \text{Var}(B\varepsilon_j) &= \mathbb{E} [|\hat{\varepsilon}(\omega_1)|^2 |\hat{\varepsilon}(\omega_2)|^2 |\hat{\varepsilon}(\omega_2 - \omega_1)|^2] \\ &\leq \mathbb{E} [|\hat{\varepsilon}(\omega_1)|^6]^{\frac{1}{3}} \mathbb{E} [|\hat{\varepsilon}(\omega_2)|^6]^{\frac{1}{3}} \mathbb{E} [|\hat{\varepsilon}(\omega_2 - \omega_1)|^6]^{\frac{1}{3}} \lesssim \sigma^6, \end{aligned}$$

and we thus obtain

$$\mathbb{E} \left[\left\| \frac{1}{M} \sum_{j=1}^M B\varepsilon_j(\omega_1, \omega_2) \right\|_{L^2(\Omega)}^2 \right] \lesssim \frac{\sigma^6}{M} |\Omega|.$$

We now bound the last three terms, starting with $\mathbb{E} [\|B_1\|_{L^2(\Omega)}^2]$. Consider the random variable

$$A_j = \hat{f}_j(\omega_1) \hat{\varepsilon}_j^*(\omega_2) \hat{\varepsilon}_j(\omega_2 - \omega_1).$$

Then

$$\begin{aligned} \mathbb{E} [\|B_1\|_{L^2(\Omega)}^2] &\lesssim \mathbb{E} \left[\left\| \frac{1}{M} \sum_{j=1}^M A_j - h(\omega_1) \mu(\omega_1) \right\|_{L^2(\Omega)}^2 \right] \\ &\quad + \mathbb{E} [\|h(\omega_1) \mu(\omega_1) - h(\omega_1) \tilde{\mu}(\omega_1)\|_{L^2(\Omega)}^2]. \end{aligned}$$

Since $\mathbb{E}[A_j] = h(\omega_1) \mu(\omega_1)$,

$$\mathbb{E} \left[\left\| \frac{1}{M} \sum_{j=1}^M A_j - h(\omega_1) \mu(\omega_1) \right\|_{L^2(\Omega)}^2 \right] = \int_{\Omega} \frac{1}{M} \text{Var}[A_j] d\omega_1 d\omega_2,$$

and

$$\begin{aligned} \text{Var}(A_j) &= \mathbb{E}[|\hat{f}_j(\omega_1) \hat{\varepsilon}_j^*(\omega_2) \hat{\varepsilon}_j(\omega_2 - \omega_1)|^2] - h^2(\omega_1) \mu^2(\omega_1) \\ &\leq \mathbb{E}[|\hat{f}_j(\omega_1) \hat{\varepsilon}_j^*(\omega_2) \hat{\varepsilon}_j(\omega_2 - \omega_1)|^2] \\ &\lesssim \sigma^4 \mathbb{E}_{t,\tau} [|\hat{f}_j(\omega_1)|^2] \end{aligned}$$

Now substitute this back into the integral to get

$$\begin{aligned} \int_{\Omega} \frac{1}{M} \text{Var}[A_j] d\omega_1 d\omega_2 &\lesssim \frac{\sigma^4}{M} \int_{\Omega} \mathbb{E}_{t,\tau} [|\hat{f}_j(\omega_1)|^2] d\omega_1 d\omega_2 \\ &= \frac{\sigma^4}{M} \int_{\Omega} \mathbb{E}_{\tau} [|\hat{f}_j(\omega_1)|^2] d\omega_1 d\omega_2 \end{aligned}$$

by translation invariance of the power spectrum. Now we have

$$\begin{aligned} & \frac{\sigma^4}{M} \int_{\Omega} \mathbb{E}_{\tau} [|\hat{f}_j(\omega_1)|^2] d\omega_1 d\omega_2 \\ &= \frac{\sigma^4}{M} \mathbb{E}_{\tau} \left[\int_{\Omega} |\hat{f}_j(\omega_1)|^2 d\omega_1 d\omega_2 \right] \lesssim_{\Omega} \frac{\sigma^4}{M} \|f\|_2^2, \end{aligned}$$

where the last line follows because $\|\hat{f}_j\|_2^2 = (1 - \tau_j) \|\hat{f}\|_2^2 \leq \frac{3}{2} \|\hat{f}\|_2^2 = 3\pi \|f\|_2^2$.

For the second term,

$$\begin{aligned} & \mathbb{E} [\|h(\omega_1) \mu(\omega_1) - h(\omega_1) \tilde{\mu}(\omega_1)\|_{L^2(\Omega)}^2] \\ &= \int_{\Omega} h^2(\omega_1) \mathbb{E} [|\mu(\omega_1) - \tilde{\mu}(\omega_1)|^2] d\omega_1 d\omega_2 \\ &\lesssim \sigma^4 \int_{\Omega} \mathbb{E} [|\mu(\omega_1) - \tilde{\mu}(\omega_1)|^2] d\omega_1 d\omega_2 \\ &= \sigma^4 \int_{\Omega} \mathbb{E} \left[\left| \frac{1}{M} \sum_{j=1}^M \hat{y}_j(\omega_1) - \mu(\omega_1) \right|^2 \right] d\omega_1 d\omega_2 \end{aligned}$$

Define $Z_j = \hat{y}_j(\omega) - \mu(\omega)$. Using similar steps to before, we get

$$\begin{aligned} & \mathbb{E} [\|h(\omega_1) \mu(\omega_1) - h(\omega_1) \tilde{\mu}(\omega_1)\|_{L^2(\Omega)}^2] \\ &\lesssim \sigma^4 \int_{\Omega} \left(\frac{1}{M} \sum_{j=1}^M Z_j \right)^2 d\omega_1 d\omega_2 \\ &= \frac{\sigma^4}{M} \int_{\Omega} \text{Var}(Z_j) d\omega_1 d\omega_2 \\ &\lesssim_{\Omega} \frac{\sigma^4}{M} (\|f\|_2^2 + \sigma^2). \end{aligned}$$

Thus $\mathbb{E} [\|B_1\|_{L^2(\Omega)}^2] \lesssim_{\Omega} \frac{\sigma^4}{M} (\|f\|_2^2 + \sigma^2)$ and an identical argument can be applied to control B_2, B_3 . Combining all terms thus gives

$$\|\tilde{g}_{\sigma}\|_{L^2(\Omega)}^2 \lesssim_{\Omega} \frac{\sigma^2}{M} \|f\|_2^4 + \frac{\sigma^4}{M} \|f\|_2^2 + \frac{\sigma^6}{M}.$$